

Identification of *Carboxypeptidase of Glutamate Like-B* as a Candidate Suppressor in Cell Growth and Metastasis in Human Hepatocellular Carcinoma

Pingping Zhang,¹ David Wai Chan,² Yi Yi Zhu,¹ Jin Jun Li,¹ Irene Oi-Lin Ng,² Dafang Wan,¹ and Jianren Gu¹

Abstract **Purpose:** We have previously done large-scale cDNA transfection screening on human hepatocellular carcinoma (HCC) cells and have identified 3,806 cDNA genes that possess the ability of either stimulating or inhibiting cell growth. In this study, we characterized one of these growth suppressor genes, *carboxypeptidase of glutamate like-B* (*CPGL-B*), in HCC. **Experimental Design:** Semiquantitative reverse-transcription PCR was used to examine the expression levels of *CPGL-B*. The cellular localization and functions of *CPGL-B* were investigated by enforced expression of *CPGL-B* in HCC cells. **Results:** From our previous cDNA transfection screening, we identified a gene named *CPGL* and its isoform, *CPGL-B*. With computational analysis, *CPGL* was located at chromosome 18q22.3 and was a homologue of peptidase family M20. *CPGL* was expressed in all adult and fetal tissues, whereas its isoform, *CPGL-B*, lacking exons 3 and 4, was expressed in all fetal tissues but only in liver and placenta of adult tissues. In HCC, *CPGL-B* was frequently underexpressed (35 of 90, 38.9%) in tumorous tissues compared with the corresponding nontumorous livers. Intriguingly, the underexpression was significantly associated with the presence of venous invasion ($P = 0.018$) and tumor microsatellite formation ($P = 0.004$). Stable transfection of *CPGL-B* in SMMC7721 HCC cells showed significant inhibition in cell viability, colony formation, cell invasion, and tumor formation in nude mice. *CPGL-B* also down-regulated CXCR3, matrix metalloproteinase 11, and CD44s, which are involved in cell growth and cell migration. **Conclusions:** These findings suggest that the frequent underexpression of *CPGL-B* may be associated with cell growth and metastasis of HCC.

Hepatocarcinogenesis is a slow and multistep process, with accumulation of activation of oncogenes and/or inactivation of tumor suppressor genes (1). It is generally accepted that understanding the mechanisms in hepatocarcinogenesis through identification and characterization of oncogenes and tumor suppressor genes will help discovery of novel targets for therapies. To achieve this, we have previously established human cDNA derived from human placenta, fetus, and normal liver tissues. Through large-scale cDNA transfection into

human hepatoma cells, we have identified potential genes involved in cancer development and progression (2).

In the present study, we describe a novel putative tumor suppressor gene, *carboxypeptidase of glutamate like* (*CPGL*), and its isoform, *CPGL-B*. This novel gene has 39.5% homology to peptidase family M20 and may belong to the M20A subfamily. This family contains the well-known protein, glutamate carboxypeptidase, which has enzymatic functions in hydrolysis of folate analogues (3, 4). This is the first report of this novel gene in human hepatocellular carcinoma (HCC). Interestingly, we have also identified an isoform of *CPGL*, which we named *CPGL-B*. This isoform lacks exons 3 and 4 and is underexpressed in HCCs and its underexpression is significantly associated with tumor microsatellite formation and venous invasion, which are features of metastasis in HCC. In addition, using *in vitro* and *in vivo* assays on cell proliferation, colony formation, cell invasion, and tumor formation in nude mice, we have shown its tumor-suppressive properties.

Materials and Methods

Cell lines. LO2 and MIHA (both normal liver cell lines), SMMC7721 (TCHu13), BEL7402 (TCHu68), SPC-A1, and Bcap37 were from Cell Bank of the Chinese Academy of Sciences; SNU368 was from Korea Cell Bank; HLE (JCRB0404) and HUH7 were from Japanese Collection of Research Bioresources; and PLC/PRF/5 (CRL-8024),

Authors' Affiliations: ¹National Laboratory for Oncogenes and Related Genes, Cancer Institute of Shanghai, Jiao Tong University, Shanghai, China and ²Department of Pathology, The University of Hong Kong, Hong Kong, China
Received 5/30/06; revised 8/24/06; accepted 8/31/06.

Grant support: Joint RGC/NSFC grant of the Hong Kong Research Grants Council (N-HKU 717/02), National Natural Science Foundation of China/Research Grants Council Joint Fund (30218006), and National Key Basic Research Project of China grant 973 (2004CB518704).

The costs of publication of this article were defrayed in part by the payment of page charges. This article must therefore be hereby marked *advertisement* in accordance with 18 U.S.C. Section 1734 solely to indicate this fact.

Note: P. Zhang and D.W. Chan contributed equally to this work.

Requests for reprints: Irene Oi-Lin Ng, Department of Pathology, The University of Hong Kong, Queen Mary Hospital, Pokfulam, Hong Kong, China. Phone: 852-2855-4875; Fax: 852-2872-5197; E-mail: iolng@hku.hk.

©2006 American Association for Cancer Research.
doi:10.1158/1078-0432.CCR-06-1307

HepG2 (HB-8065), Hep3B (HB-8064), SK-Hep-1 (HTB-52), SNU182 (CRL-2235), SNU449 (CRL-2234), and SNU475 (CRL-2236) were from American Type Culture Collection (Rockville, MD). They were grown at 37°C in 5% CO₂ in MEM, DMEM, or RPMI 1640 supplemented with 10% FCS.

Patients and samples. Ninety patients who had primary HCC resected at Queen Mary Hospital (Hong Kong, China) between October 1992 and May 2001 were randomly selected. Seventy were men and 20 were women. Patients' age ranged from 24 to 74 years, with a mean age of 52 years. Sixty-seven (74.4%) of the patients were positive for hepatitis B surface antigen (HBsAg), whereas only 5 (5.6%) patients were positive for hepatitis C virus antibody and they were HBsAg negative. All samples were immediately frozen in liquid nitrogen and kept at -80°C until analysis. The nontumorous liver samples were taken away from tumors. Serum HBsAg and anti-hepatitis B surface were assayed by an enzyme immunoassay test (Abbott Laboratories, Chicago, IL). Normal liver tissues were taken from three patients who had liver resection for colonic cancer metastasis to the liver.

Plasmids and cell transfection. The full-length cDNAs of CPGL and CPGL-B were amplified by a pair of primers (Genbank accession no. AJ347717): 5'-AAGATGCGCGCCCTCACTAC-3' (sense) and 5'-CTTGGCCTAGTCCTCAGCTGGGA-3' (antisense); the characters in italics being start and stop codons, respectively, on human placental cDNA library (Clontech, Palo Alto, CA). The cDNA fragments were digested by *Kpn*I and cloned into pcDNA3.1/His-V5 expression plasmid (Invitrogen Life Technologies, Carlsbad, CA) to generate pcDNA3.1/His-V5/CPGL and pcDNA3.1/His-V5/CPGL-B constructs, respectively. To generate the pEGFP-N1/CPGL-B construct for CPGL-B localization experiment, the CPGL-B cDNA was amplified by a set of primers (Genbank accession no. AJ347717): 5'-GGAATTCAGATGCGCGCCCTCACTACC-3' (sense); 1-18 bp with additional *Eco*R1 site before start codon) and 5'-CGGGATCCTCCTCAGCTGGGAGACTC-3' (antisense); 1,405-1,424 bp with modified stop codon into *Bam*HI site). The cDNA fragment was digested by *Eco*R1 and *Bam*HI and cloned into pEGFP-N1 plasmid (Clontech). All the sequences of the cDNA fragments and their ligation sites in constructs were confirmed by sequencing analysis.

Cell transfection was carried out by plating 2 × 10⁵ SMMC7721 cells on 35-mm Petri dishes and transfected with 2 μg constructs by LipofectAMINE 2000 according to the manufacturer's instructions (Invitrogen Life Technology). The empty pcDNA3.1/His-V5 vector was used as a mock control. The transfected cells were selected by G418 at 400 μg/mL for 2 weeks. Resistant clones were randomly chosen for cell number expansion to establish stably expressing clones.

RNA extraction and reverse-transcription PCR analysis. Total RNA from each cell line was prepared by Trizol reagent (Invitrogen) and treated by DNaseI (Promega, Madison, WI) according to the manufacturer's instructions. To do semiquantitative reverse-transcription PCR (RT-PCR), the first-strand cDNA was synthesized from 2 μg total RNA using GeneAmp RNA PCR kit components (Applied Biosystems, Foster City, CA). The CPGL and CPGL-B mRNA levels were detected by semiquantitative RT-PCR using a pair of primers [Genbank accession no. AJ347717; 5'-GAGAAGAGAGGCCAAATCAG-3' (P1; 106-129 bp) and 5'-CAGAGCCTGACTCCTCCATG-3' (P2; 492-511 bp)] and with the following conditions for 33 cycles: denaturation at 94°C for 30 seconds, annealing at 54°C for 30 seconds, and extension at 72°C for 50 seconds. As the copy number of CPGL is higher than CPGL-B, the number of PCR cycles was set to 28 cycles for semiquantitative RT-PCR on CPGL mRNA in HCC samples and cell lines. The *glyceraldehyde-3-phosphate dehydrogenase* mRNA was used as internal control amplified by the following primers [Genbank accession no. BC083511; 5'-ACGGATTGGTCGTATTGGG-3' (sense; 26-45 bp) and 5'-TGATTTGGAGGGATCTCCG-3' (antisense; 237-256 bp)] and with amplification at 22 cycles: denaturation at 94°C for 30 seconds, annealing at 55°C for 30 seconds, and extension at 72°C for 1 minute. The PCR products were separated by 2% agarose gel with

ethidium bromide and gel image was captured by AlphaImager imaging system (Alpha Innotech, San Leandro, CA). Band intensity was measured by the software from AlphaImager imaging system. The relative gene expression levels of both CPGL and CPGL-B were normalized by *glyceraldehyde-3-phosphate dehydrogenase*. The relative expression level of CPGL-B of tumorous liver sample was compared with that of corresponding nontumorous liver sample. A ratio of tumorous liver sample/nontumorous liver sample mRNA of ≤0.5-fold was defined as underexpression, whereas a ratio of ≥2-fold was defined as overexpression of CPGL-B in HCC.

Northern blot analysis on human tissues was done using CPGL cDNA as a probe on a commercial human normal tissues membrane (Clontech). Prehybridization and hybridization were carried out at 68°C in 1% SDS, 1 mol/L NaCl, and 10% dextran sulfate solution. The CPGL cDNA probe was labeled with [α -³²P]dCTP using the random primer labeling kit (Promega). After the washing procedure, RNA blots were exposed to phosphoimage screen and then read out using Molecular Imager FX and software Quantity One (Bio-Rad, Hercules, CA).

Protein extraction and Western blot analysis. Protein extracts were prepared from lysis of harvested cells by radioimmunoprecipitation assay buffer [50 mmol/L Tris-Cl (pH7.4), 150 mmol/L NaCl, 1% Triton X-100, 0.1% SDS, 1% sodium deoxycholate, 1 mmol/L EDTA] supplemented with 5 mmol/L NaF, 2 μg/mL pepstatin A, 2 μg/mL aprotinin, and 2 μg/mL leupeptin for 30 minutes at 4°C. For Western blot analyses, 25 μg each protein samples were separated by SDS-PAGE and electroblotted onto Hybond-P membranes (Amersham Pharmacia Biotech, Cleveland, OH). Blots were blotted with 5% skim milk followed by incubation with antibodies specific for anti-CXCR3 (1:4,000 dilution; Sigma, Saint Louis, MO), anti-matrix metalloproteinase (MMP) 11 (1:1,000 dilution; Sigma), anti-CD44s (1:4,000 dilution; Sigma), and anti-V5 (1:4,000 dilution; Invitrogen). The rabbit anti-CPGL-B polyclonal antibody was generated by the Cancer Institute of Shanghai, Jiao Tong University (Shanghai, China). Briefly, CPGL-B full-length cDNA was subcloned into PT7-470 6xHis-tagged expression vector. CPGL-B protein was purified through affinity chromatography column with ligand of 6xHis tag and identified by SDS-PAGE and Western blot analysis. Rabbits were immunized with CPGL-B protein for four times and specific anti-serum was harvested 6 weeks after immunization. The specificity of the polyclonal anti-CPGL-B antibody from the immunized rabbit was tested with Western blotting (1:1,000 dilution). Blots were then incubated with donkey anti-goat, anti-rabbit, or anti-mouse secondary antibody conjugated to horseradish peroxidase (Amersham Pharmacia Biotech).

Immunocytochemistry. Stable clones of CPGL-B-expressing and vector control-expressing SMMC7721 cells were grown on glass slide in culture medium for overnight. Cells were then fixed by acetone and permeabilized by 0.1% Triton X-100 in PBS before blocking the endogenous peroxidase with 0.3% H₂O₂ in methanol and nonspecific binding sites with 3% bovine serum albumin in PBS. After removing the blocking solutions, cells on the glass slides were then immunostained with a panel of antibodies consisting of CXCR1, CXCR2 (both from R&D Systems, Minneapolis, MN), CXCR3 (Sigma), CXCR4, CXCR5, CXCR6 (all from R&D Systems), MMP2, MMP9 (both from Santa Cruz Biotechnology, Santa Cruz, CA), MMP11 (Sigma), ANG1, ANG2, OPN, integrin β₃, integrin β₅, integrin α_vβ₃, HIF1α (all from Santa Cruz Biotechnology), nm23 (DAKO, Glostrup, Denmark), and CD44s (Sigma). For negative controls, the primary antibody was replaced with TBS. Protein signals were developed with 3,3'-diaminobenzidine (Sigma) substrate solution and then counterstained with Mayer's hematoxylin, dehydrated with ethanol, and fixed with xylene and mounted slides with coverslips.

Cell viability assay. The cell viability of CPGL-B-transfected SMMC7721 cells was examined by 3-(4,5-dimethylthiazol-2-yl)-2,5-diphenyltetrazolium bromide (MTT) assay. The transfected cells (mock control and CPGL-B-transfected cells) were plated in 96-well microtiter plates at a density of 1 × 10⁴ per well. They were further cultured for

24, 48, 72, 96, 120, and 144 hours, after which the medium was replaced with 100 μ L fresh serum-free medium containing 50 μ g MTT. Three hours later, the color reaction was quantified with an ELISA plate reader (Bio-Rad) at a test wavelength of 570 nm and a reference wavelength of 630 nm. The cell viability rates for the cell lines transfected with CPGL-B and mock control were compared. The entire experiment was done thrice independently.

Cell cycle and cell apoptosis analyses. The cell cycle of cells was determined by fluorescence-activated cell analysis of propidium iodide-stained cells on a FACSCalibur flow cytometer (Becton Dickinson, San Jose, CA). Cells were synchronized to G₂-M by pretreatment of nocodazole (0.2 μ g/mL) for 20 hours and then washed with PBS and fixed with cold 70% ethanol for at least an hour. Before flow cytometric analysis, cells were incubated with 200 μ L DNase-free RNaseA at 200 μ g/mL and propidium iodide at 1 mg/mL at 37°C for 30 minutes. A total of 10⁴ cells were analyzed for each sample. Cell cycle analysis was done using the Multicycle software (Beckman Coulter, Fullerton, CA). The cell apoptosis was determined by Annexin V-FITC Apoptosis Detection kit according to the manufacturer's protocol (BD Biosciences, San Jose, CA).

Colony formation assay. The colony formation ability of CPGL-B in SMMC7721 cells was evaluated by transfecting 1 μ g pcDNA3.1/His-V5/CPGL-B into SMMC7721 cells (5 \times 10⁴ per well) in six-well plate using LipofectAMINE kit (Invitrogen). The pcDNA3.1/His empty vector was used to generate the mock control. Each transfection was done in triplicate. The transfected cells were selected by G418 at 400 μ g/mL for 2 weeks. The resistant colonies were stained by Coomassie blue (Sigma) and then scored. The above experiment was done at least thrice and the data were expressed as mean \pm SD.

Matrigel invasion assay. Cell invasion was quantified *in vitro* using Transwell chambers with polycarbonate membrane filters (8- μ m pore size) coated with a Matrigel gel (Becton Dickinson Biosciences Discovery Labware, Bedford, MA). Briefly, 1 \times 10⁵ CPGL-B stably expressing cells or empty vector control cells were washed by DMEM twice before seeding in triplicate in the inner chamber of the insert containing 300 μ L serum-free medium. Five hundred microliter of medium containing 10% fetal bovine serum were added to the lower chamber. The plates were incubated for 20 hours at 37°C. Then, the noninvading cells from the interior of the inserts were gently removed using a cotton-tipped swab. The invasive cells that migrated from the upper to the lower surface of the membrane were stained and three fields of the invading cells were counted under the microscope at \times 400 magnification for replicate Transwells and captured by photographing. The experiment was done thrice independently.

Tumorigenicity assay in nude mice. The tumor formation ability of CPGL-B-transfected SMMC7721 cells was evaluated by injecting cell suspensions into BALB/c *nu/nu* female mice. For each mouse, 2.5 \times 10⁵ cells of each cell line (CPGL-B- or vector-transfected SMMC7721 cells) were injected s.c. into both flanks. After 6 to 7 weeks, mice were sacrificed and each tumor was dissected out for weighing. Each experimental group consisted of six mice and the experiment was repeated twice. All the animal experiments were done with approval and conformed to United Kingdom Coordinating Committee on Cancer Research guidelines for the welfare of animals in experimental neoplasia.

Computational analysis. The sequences of CPGL and CPGL-B were analyzed and blasted by using the Genbank data at the National Center for Biotechnology Information (NCBI) with BLAST program.³

Clinicopathologic analysis. The clinicopathologic features of patients analyzed in this study included tumor size, cellular differentiation, presence of venous invasion, tumor microsatellite formation, direct invasion into the adjacent liver parenchyma, tumor stage (pTNM stage), and serum HBsAg status. They were analyzed as described previously (5).

Statistical analysis. Statistical analysis was done with SPSS for Windows version 14.0 (SPSS, Inc., Chicago, IL). Fisher's exact or χ^2 test was used for statistical analysis of categorical data. All *P* values were two tailed and considered significant when they were <0.05.

Results

Identification of CPGL and its isoform CPGL-B. From our previous large-scale cDNA transfection screening (2), we isolated a 1.6-kb cDNA fragment from our laboratory's cDNA library. By 5' rapid amplification of cDNA ends, an additional 1.7-kb cDNA fragment of 5' end was obtained. Combining these two cDNA fragments, we obtained a full-length cDNA of 2,364 bp, which we designated PP856 (Genbank accession no. AF258592). With further RT-PCR on the same cDNA library, we obtained another cDNA fragment, which was 252 bp longer than PP856, and we named it CPGL (Genbank accession number. AJ347717), whereas PP856 was renamed CPGL-B. With sequence analysis, the full length of CPGL was found to be 2,616 bp and predicted to encode 475 amino acids with a size of 52.8-kDa, whereas the full length of CPGL-B was 2,364 bp and predicted to encode 391 amino acids with a size of 43.8 kDa (Fig. 1A). Both cDNA fragments have complete 5' and 3' end signals, and their cDNA sequences were identical in placental and adult liver tissues, according to the analysis result from Human Genome Bank Blast. The transcriptional start site follows Kozak rule (A/GNNATG; ref. 6). CPGL encodes 11 exons, and CPGL-B encodes 9 exons, lacking 252 bp and without exons 3 and 4 (Fig. 1A). All exon/intron boundaries conform to the Breathnach (GT/AG) rule (7) and all splice donor and acceptor sites conform to Mount's consensus sequence (8). Because CPGL-B just lacks exons 3 and 4, compared with CPGL, we regard CPGL-B as an isoform of CPGL as a result of alternative splicing.

Besides, with the Human Genomic Blast program at the NCBI, CPGL was localized to chromosome 18q22.3. Using the software of protein-protein BLAST and the conserved domain database from the NCBI, we found that the NH₂ terminus from 1 to 326 amino acids of CPGL had 39.5% homology with the conserved region of peptidase family M20 (Fig. 1B). However, CPGL-B lacks 84 amino acids at the NH₂ terminus of CPGL (318-570 bp; Fig. 1A), the 68 amino acids of which encode the peptidase M20 functional domain (Fig. 1B). The absence of this domain indicates it is likely that CPGL-B does not have the same functions of peptidase family (9).

Expression patterns of CPGL and CPGL-B in human normal tissues. To analyze the expression of CPGL in human normal tissues, we did Northern blot analysis on a commercial human normal tissues membrane (Clontech), using CPGL cDNA as a probe (Fig. 1C). The results revealed that CPGL transcript was ubiquitously expressed in all human adult and placental tissues, with higher levels in kidney and liver, but was not detectable in peripheral blood lymphocytes (Fig. 1C). As CPGL-B is only 252 bp shorter than CPGL, we could not use the same membrane to analyze the expression of CPGL-B. To solve this problem, we used RT-PCR analysis with a pair of specific primers for both CPGL and CPGL-B on various human fetal, adult, and placental tissues. CPGL was ubiquitously expressed in all human fetal tissues and human adult tissues. Interestingly, CPGL-B, unlike CPGL, showed a more restricted expression pattern. Although CPGL-B was expressed in all human fetal tissues analyzed (Fig. 1D), it was only expressed in

³ www.ncbi.nlm.nih.gov.

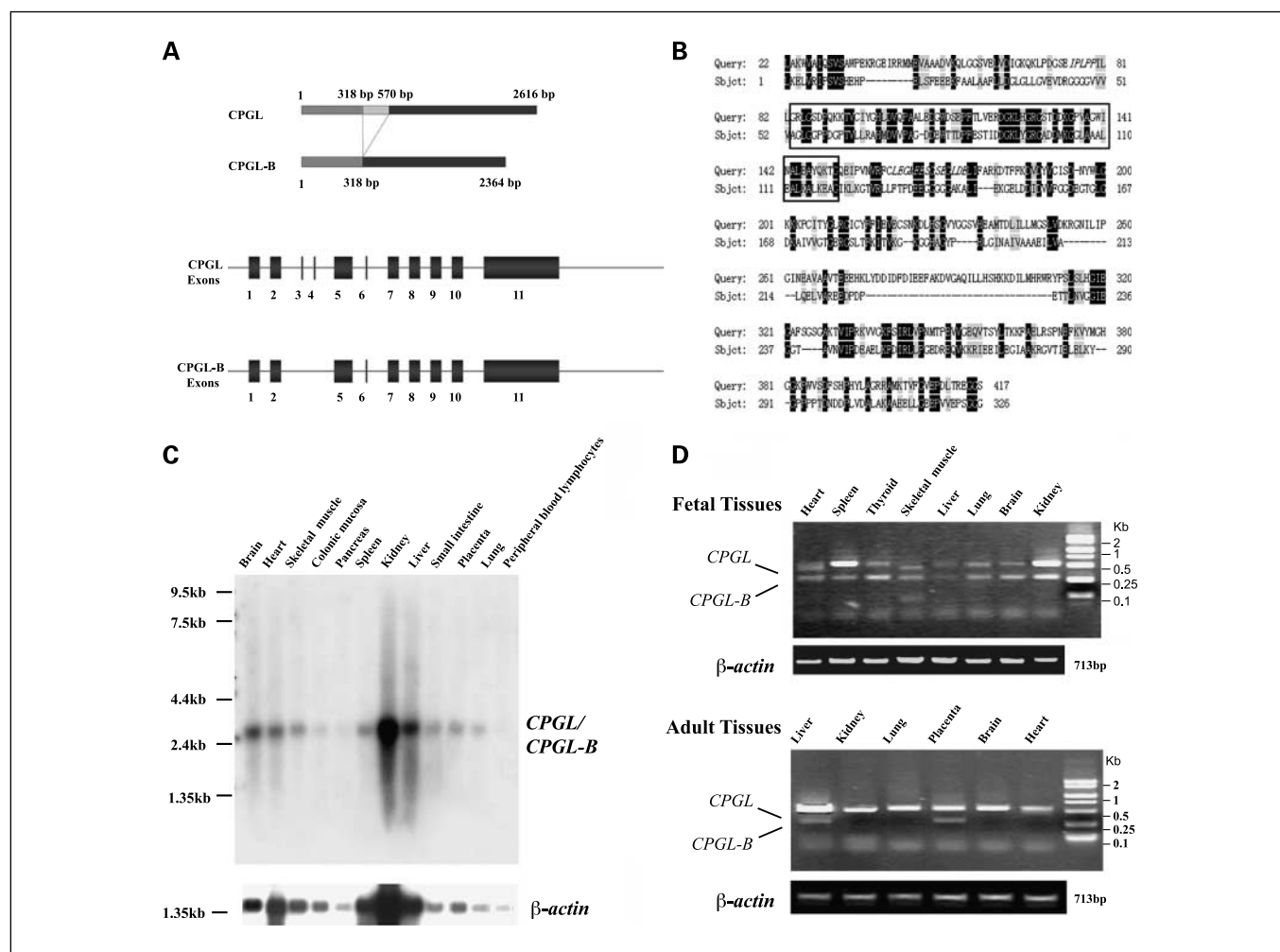


Fig. 1. Genome structure, chromosomal localization, expression patterns of human *CPGL* and *CPGL-B*. **A**, two alternative structures of *CPGL*, *CPGL*, and *CPGL-B*. *CPGL* is 252 bp longer than *CPGL-B* because of the absence of exons 3 and 4 in *CPGL-B*. **B**, *CPGL* is a homologue of peptidase family M20. From the database of NCBI Web site, *CPGL* was found to have 39.5% homology to peptidase family M20. Query, peptidase family M20; subject, *CPGL*. Rectangular box, peptidase M20 functional domain. **C**, Northern analysis of human adult tissues probed with human *CPGL* cDNA. Single *CPGL* transcript. **D**, semiquantitative RT-PCR analysis of *CPGL-B* in human fetal tissues (*top*) and adult and placental tissues (*bottom*). The upper band with heavier molecular weight is *CPGL*, whereas the lower band is *CPGL-B*. β -Actin was used as the internal control.

human adult liver and placental tissues (Fig. 1D). The results showed that *CPGL* and *CPGL-B* had different expression patterns in human adult tissues.

Analysis of expression of *CPGL-B* in human HCC, HCC cell lines, and normal liver tissues. As *CPGL* was highly expressed and *CPGL-B* was uniquely expressed in human adult liver tissue, we examined their expression status in primary HCC tissue samples with semiquantitative RT-PCR analysis. Of the 90 paired HCC samples, 35 (38.9%) HCCs were found to have either no or little *CPGL-B* mRNA compared with their corresponding nontumorous liver tissues (Fig. 2A). Six (6.7%) HCCs had higher *CPGL-B* mRNA levels than their corresponding nontumorous liver tissues and the other 49 (54.4%) showed equal expression levels of *CPGL-B* in both tumorous and nontumorous tissues. However, for *CPGL*, there was no significant difference in its expression levels between HCCs and their corresponding nontumorous livers. Both *CPGL* and *CPGL-B* were expressed in the three normal liver tissues (Fig. 2A).

We also examined the expression levels of *CPGL-B* in human immortalized normal liver and HCC cell lines. *CPGL-B* was clearly expressed in two immortalized normal liver cell lines (LO2 and MIHA), whereas its expression was either little or absent in the 11 HCC cell lines (Fig. 2B). By Western blot analysis, *CPGL-B* protein levels in HUH7, Hep3B, HepG2, BEL7402, and SMMC7721 were relatively lower compared with the immortalized normal liver cell line, LO2 (Fig. 2C).

Clinicopathologic correlation. On clinicopathologic correlation, *CPGL-B* underexpression (≥ 2 -fold) in HCCs was significantly associated with the presence of venous invasion ($P = 0.018$) and tumor microsatellite formation ($P = 0.004$; Table 1). There was, however, no association between underexpression of *CPGL-B* and tumor size, encapsulation, cellular differentiation, tumor stage, and HBsAg status.

Inhibition of cell viability, cell invasion, and tumorigenicity of HCC cells by *CPGL-B*. To investigate if *CPGL-B* had tumor-suppressive activity, we stably transfected *CPGL-B* into SMMC7721 cells and examined its effects on cell viability using

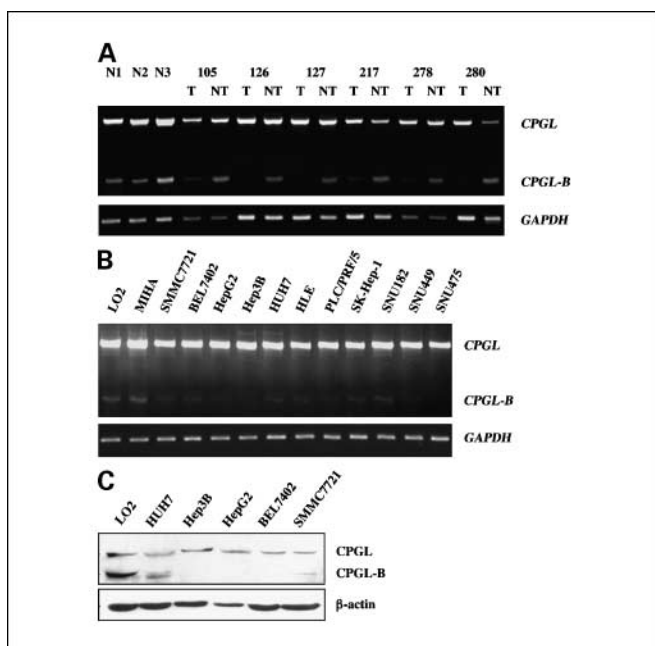


Fig. 2. The expression levels of CPGL-B in HCC clinical samples and cell lines. Semiquantitative RT-PCR showed the expression of *CPGL-B* and *CPGL* in human normal liver tissues and HCC samples. T, tumorous tissue; NT, corresponding nontumorous tissue; N1, N2, and N3, normal liver tissues (A). Expression of *CPGL-B* and *CPGL* in human normal liver cell lines (LO2 and MIHA) and human HCC cell lines (B). Western blot analysis showed the levels of CPGL and CPGL-B protein levels in human normal liver cell line, LO2, and human HCC cell lines (C).

MTT assay (Fig. 3A). After the cells were transfected with pcDNA3.1/His-V5/CPGL-B, significant inhibition on cell viability was observed on day 4 and persisted until day 6 compared with the mock control ($P < 0.01$ at all time points on days 4, 5,

and 6; Fig. 3A). To examine long-term cell proliferation, we next did colony formation assay by transiently transfecting CPGL-B-expressing vector into SMMC7721 cells. As compared with empty vector control, a significant reduction in the colony formation ability was seen in the SMMC7721 cells transfected with pcDNA3.1/His-V5/CPGL-B ($P < 0.05$; Fig. 3B).

With flow cytometric analysis, we found that higher proportions of CPGL-B-transfected SMMC7721 cells ($82 \pm 0.4\%$) were at the G_1 phase than the vector control ($24.8 \pm 1.73\%$; Fig. 3C). Besides, with Annexin V-FITC Apoptosis Detecting kit and flow cytometric analysis, more apoptotic cells were found in CPGL-B-transfected SMMC7721 cells ($33.24 \pm 1.41\%$) than the vector control ($17.77 \pm 1.2\%$; Fig. 3D). These data suggest that CPGL-B inhibits cell growth by inducing G_1 arrest and sensitizing SMMC7721 cells to apoptosis.

We next tested the effect of CPGL-B on HCC cell invasion using Matrigel invasion assay. SMMC7721 cells with CPGL-B expression showed $>50\%$ inhibition on cell invasion activity compared with the empty vector control ($P < 0.002$; Fig. 4A). We further examined whether CPGL-B could suppress the tumorigenic activity of HCC cells by evaluating tumor development in nude mice. Cells from one of CPGL-B stably expressing SMMC7721 clones and the vector control-transfected SMMC7721 cells were inoculated into nude mice, respectively. At 7 weeks after inoculation, the mean tumor weight of vector control was 0.55 ± 0.16 g. In contrast, the CPGL-B clone showed significantly reduced tumor size by $>50\%$, with mean tumor weight being 0.26 ± 0.07 g (Fig. 4B). In contrast, when CPGL-B was stably transfected into other human cancer cell lines, SPC-A1 (lung carcinoma) and Bcap37 (breast cancer), no difference was found in the colony formation ability compared with vector control (data not shown). Therefore, these data indicate that CPGL-B is able to inhibit tumorigenic activity specifically in HCC cells.

Table 1. Clinicopathologic correlation of CPGL-B expression in human HCC

Variables	Underexpression of CPGL-B (≥ 2 -fold), n (%)	Normal expression, n (%)	P
Tumor microsatellite formation			
Present	26 (76.5)	24 (43.6)	0.004*
Absent	8 (23.5)	31 (56.4)	
Venous invasion			
Present	25 (71.4)	25 (45.5)	0.018*
Absent	10 (28.6)	30 (54.5)	
Cellular differentiation (by Edmondson)			
Grades 1 and 2	7 (24.1)	22 (46.8)	0.056
Grades 3 and 4	22 (75.9)	25 (53.2)	
Tumor size (cm)			
< 5	7 (24.1)	20 (42.6)	0.140
> 5	22 (75.9)	27 (57.4)	
Tumor stage			
I and II	7 (25)	19 (41.3)	0.210
III and IV	21 (75)	27 (58.7)	
Tumor Encapsulation			
Present	9 (25.7)	22 (40.7)	0.176
Absent	26 (74.3)	32 (59.3)	
Serum HBsAg			
Present	25 (75.8)	42 (77.8)	1.000
Absent	8 (24.2)	12 (22.2)	

* $P < 0.05$.

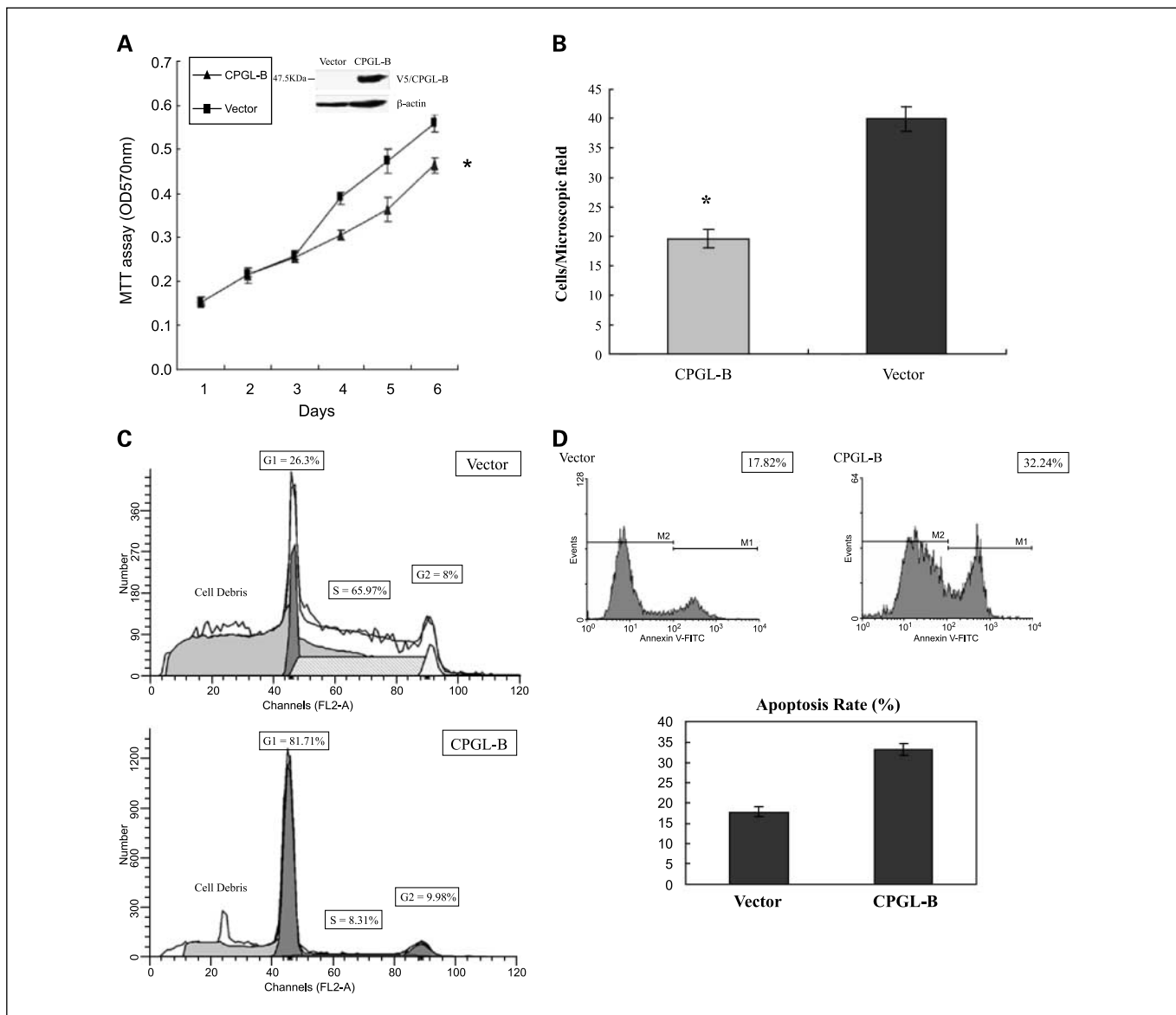


Fig. 3. Enforced expression of CPGL-B reduced cell viability, induced G₁ arrest, and increased cell apoptosis in SMMC7721 cells. **A**, CPGL-B decreased cell viability of SMMC7721 cells as shown by MTT assay. *, $P < 0.01$ for all time points from days 4 to 6. The expression levels of transfected CPGL-B in SMMC7721 cells are shown by Western blotting. **B**, CPGL-B inhibited colony formation of SMMC7721 cells. Cell lines used in this experiment were SMMC7721 cells transfected with either CPGL-B or empty vector pcDNA3.1. Data were counted in triplicate in at least three independent experiments. Columns, mean; bars, SD. *, $P < 0.05$. **C**, CPGL-B induced G₁ cell cycle arrest in SMMC7721 cells. Results are representative of one of the three independent experiments and show the corresponding cell cycle distribution of the cells (in percentages) of the CPGL-B transfectants and empty vector pcDNA3.1. **D**, CPGL-B increased apoptosis of SMMC7721 cells. Top, apoptotic cells were stained by using the Annexin V-FITC Apoptosis Detection kit and analyzed by flow cytometry. Top right corner, percentage of AnnexinV-FITC – positive cells. M1, Annexin V-FITC positive and propidium iodide negative; M2, Annexin V-FITC and propidium iodide negative. Bottom, results of three independent experiments.

Cytoplasmic localization of CPGL-B. To study the subcellular localization CPGL-B, CPGL-B was fused to enhanced green fluorescent protein (EGFP) expression vector. With transient transfection in SMMC7721 cells and observation under fluorescence microscope, EGFP-CPGL-B (Fig. 4C) was found to localize mainly in the cytosol.

Down-regulation of cell migration factors by CPGL-B. Because the experiments above showed that CPGL-B localized in cytoplasm and exhibited inhibition of cell growth, suppressed cell migration, and reduced tumorigenic activity, we sought to investigate if CPGL-B affected expression of genes that are involved in cell migration, invasion, and growth. A wide range of

well-known genes (*CXCR1*, *CXCR2*, *CXCR3*, *CXCR4*, *CXCR5*, *CXCR6*, *MMP2*, *MMP9*, *MMP11*, *ANG1*, *ANG2*, *OPN*, *integrin β_3* , *integrin β_5* , *integrin $\alpha_v\beta_3$* , *nm23*, *CD44s*, and *HIF1 α*) associated with cancer cell migration and survival were evaluated by immunocytochemistry on CPGL-B and empty vector-transfected SMMC7721 cells. Three of these genes, *CXCR3*, *MMP11*, and *CD44s*, which are frequently overexpressed in many human cancers and are involved in cell migration and cell growth (10–12), were found to be down-regulated in CPGL-B-transfected SMMC7721 cells by immunohistochemistry (Table 2). Western blot analysis further validated that the expression levels of *CXCR3*, *MMP11*, and *CD44s* were remarkably

down-regulated in CPGL-B-transfected SMMC7721 cells compared with the parental cells and vector control (Fig. 4D).

Discussion

In our previous large-scale cDNA transfection study on human hepatoma cells (2), we have identified a significant number of potential genes, which may be involved in HCC development and progression. In the present study, we have further characterized a putative tumor suppressor gene in HCC, *CPGL-B*, an isoform of *CPGL*, among these potential genes.

CPGL is a novel gene not reported previously and has unknown functions. However, with its high sequence homology with peptidase family M20, it has been classified as Metrops ID M20.005, and we have designated it as *CPGL*. The enzymes of the M20 family have different potential applications (13), but the defined functions of each member are unclear and currently under investigations. Glutamate carboxypeptidase is one of the well-known enzymes generated from *Pseudomonas* species and has the enzymatic hydrolysis of folate

analogues (3). As *CPGL* shares a high homology with this family, it is likely that it contains some similar functions like glutamate carboxypeptidase. However, further investigations on the enzymatic activities of *CPGL* are needed.

CPGL-B is an alternative isoform of *CPGL* with absence of exons 3 and 4 encoding the peptidase M20 functional domain. The alteration of the NH₂ terminus of *CPGL-B*, compared with *CPGL*, implies that this isoform lacks peptidase M20 enzymatic activity and may function differently from *CPGL*. Indeed, with RT-PCR and Northern blot analyses, *CPGL* was found to be expressed in all human fetal and adult tissues. However, *CPGL-B* was expressed in all fetal tissues, but in adult tissues, it was expressed only in liver and placenta. This suggests that the role of *CPGL-B* is likely to be different from that of *CPGL*. *CPGL-B* may play important roles during fetal development, but subsequently, its expression is lost in most of the adult tissues except liver. This further indicates that *CPGL-B* may be particularly important in the maintenance of cellular functions in adult liver tissue. In addition, transfection *CPGL-B* into HCC cells resulted in significant induction of G₁ arrest, sensitization

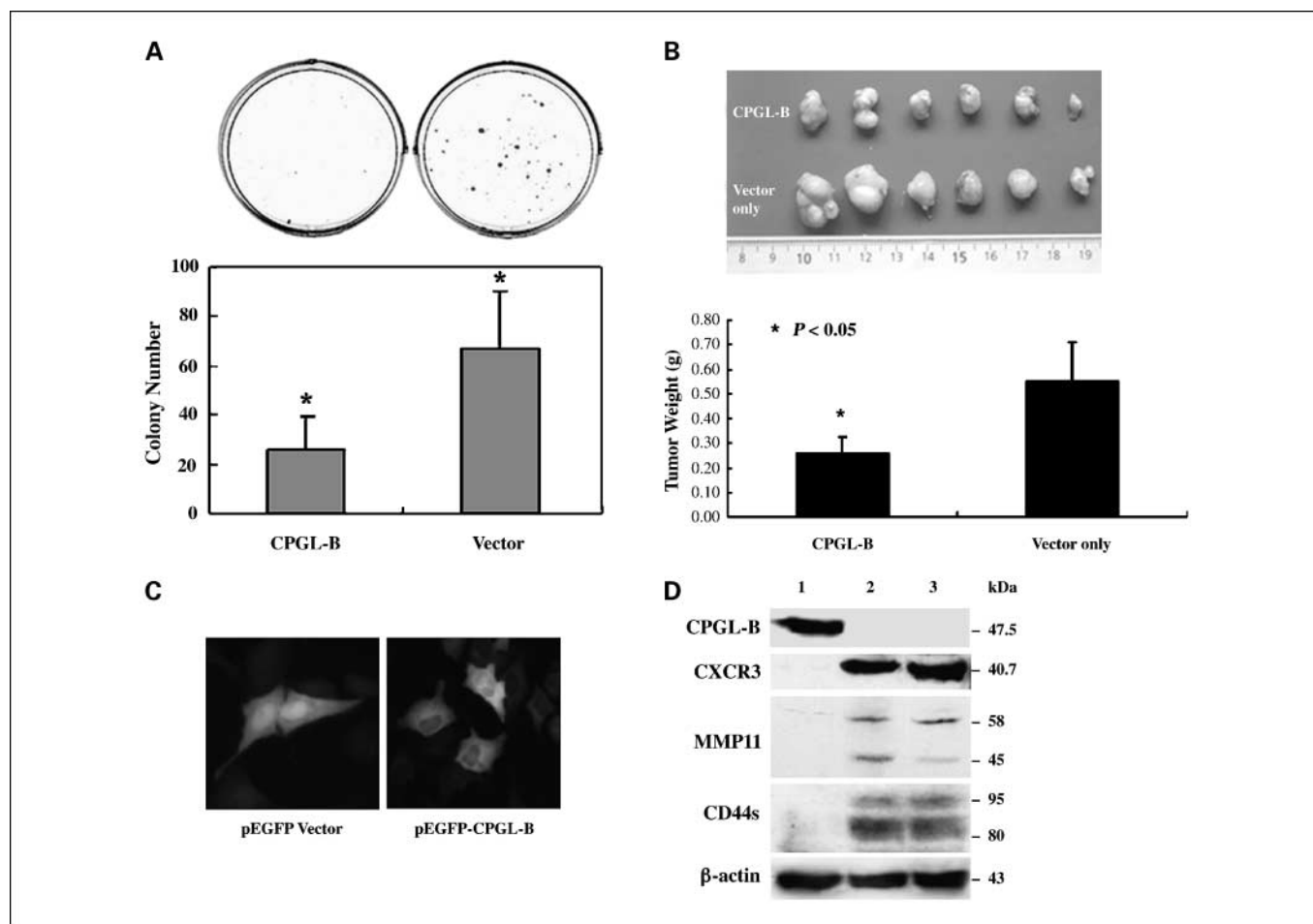


Fig. 4. Localization and effects of CPGL-B on cell migration factors and tumorigenicity of SMMC7721 cells. **A**, Transwell invasion assay of SMMC7721 cells transfected with *CPGL-B* and empty vector. Data are expressed as the mean number of cells counted in three fields in replicate Transwells from one experiment. Columns, mean; bars, SD. *, $P < 0.002$. **B**, CPGL-B inhibited tumor formation in nude mice. Nude mice were inoculated with SMMC7721 cells stably transfected with empty vector and CPGL-B expression vectors, and tumors were analyzed at weeks 6 to 7. Columns, mean tumor weight; bars, SE. All the tumor weight measurements were done at weeks 6 to 7. *, $P < 0.002$. **C**, intracellular localization of recombinant CPGL-B was determined by whole-cell fluorescence by transfecting pEGFP/*CPGL-B* vector in SMMC7721 cells. pEGFP-N1 vector was used as control. The images were visualized with fluorescence microscopy. **D**, Western blot analysis showed that overexpression of CPGL-B down-regulated CXCR3, MMP11, and CD44s in SMMC7721 cells. Lane 1, *CPGL-B*-transfected SMMC7721 cells; lane 2, vector control; lane 3, SMMC7721 parental cells.

Table 2. Immunocytochemical analysis on the expression patterns of some known metastasis-related proteins in *CPGL-B*-transfected and empty vector-transfected SMMC7721 cells

Antibody (dilutions)/sources	pcDNA3.1/His-V5	pcDNA3.1/His-V5/ <i>CPGL-B</i>
CXCR1 (1:25)/m	–	–
CXCR2 (1:25)/m	–	–
CXCR4 (1:25)/m	–	–
CXCR5 (1:25)/m	–	–
CXCR6 (1:25)/m	–	–
MMP2 (1:25)/r	–	–
MMP9 (1:50)/g	+	+
ANG1 (1:100)/g	+++	+++
ANG2 (1:100)/g	++++	++++
OPN (1:100)/g	+++	+++
Integrin β_3 (1:50)/g	++	+
Integrin β_5 (1:50)/r	+	++
Integrin $\alpha_v\beta_3$ (1:10)/m	–	+
HIF1 α (1:25)/r	–	–
nm23 (1:10)/r	+	+
CXCR3 (1:25)/m*	+++	+
MMP11 (1:50)/g*	+++	+
CD44s (1:25)/m*	++++	+

NOTE: “–” and “+” indicate absence and presence of expression level, respectively. The number of “+” represents expression levels. Antibody sources are the following: mouse (m), rabbit (r), and goat (g).

*Metastasis-related proteins remarkably down-regulated in *CPGL-B*-transfected SMMC7721 cells.

to cell apoptosis, inhibition of cell growth, and tumor formation in nude mice. In contrast, *CPGL-B* could not inhibit tumorigenicity of other human cancer cells, such as SPC-A1 and Bcap37. This indicates that *CPGL-B* has cellular functions specifically in HCC cells. Furthermore, the inhibition on cell invasion of SMMC7721 by *CPGL-B* as shown by Matrigel invasion assay suggests that this gene has suppressive effects on cell invasion and metastasis. Indeed, this result was in accordance with our clinicopathologic finding that underexpression of *CPGL-B* in HCCs was associated with venous invasion and tumor microsatellite formation, which are established features of tumor metastasis in HCC. Therefore,

our data strongly suggest that *CPGL-B* has tumor and metastasis suppressive functions. Its restrictive expression in normal adult liver, underexpression in human HCCs, and significant tumor-suppressive activity implicate that it is a putative tumor suppressor gene and may play an important role in HCC development. However, how *CPGL-B* mediates this tumor-suppressive function remains unclear.

Although there is no information on which signaling pathways *CPGL-B* is involved in at present, the down-regulation of *CXCR3*, *MMP11*, and *CD44s* by *CPGL-B* at protein level raised a suggestion that *CPGL-B* might interact with these genes in modulating cell migration and growth in HCC cells. *CXCR3* is a member of the chemokine receptors eliciting cell migration responses and activation of several signaling pathways expressed in metastatic cancers (12, 14–19). *MMP11* belongs to the stromelysin subgroup of MMPs that is up-regulated in invasive cancer and is able of preventing cancer cell death through apoptosis and necrosis (11, 20, 21). In addition, *CD44s* is the standard isoform of *CD44*, which is a membrane receptor implicated in cell adhesion, motility, and metastases and has shown overexpression in many human cancers for modulating cell migration and invasion (10, 22–25). All of these three factors are key players during cancer development, progression, and metastases. Therefore, the down-regulation of these three factors by *CPGL-B* implicates a mechanistic relationship, whether direct or indirect, in HCC cells.

In summary, in this study, we have identified a novel gene, *CPGL*, and its isoform, *CPGL-B*. We have shown that *CPGL-B* was frequently underexpressed in human HCCs and the underexpression was significantly associated with venous invasion and tumor microsatellite formation. It also possessed tumor- and metastasis-suppressive activities in HCC cells. With *in vitro* and *in vivo* tumorigenic assays, *CPGL-B* was able to reduce cell growth, inhibit colony formation and cell invasion activity, and suppress tumor formation in nude mice. Its down-regulation of *CXCR3*, *MMP11*, and *CD44s* suggests that *CPGL-B* might interact with them in controlling cell growth and cell migration. The overall findings suggest that *CPGL-B* plays an important role in HCC and may be a putative tumor suppressor gene in hepatocarcinogenesis. Further understanding of the molecular pathways related to *CPGL-B* in regulating carcinogenesis would be useful.

References

- Nowell PC. Mechanisms of tumor progression. *Cancer Res* 1986;46:2203–7.
- Wan D, Gong Y, Qin W, et al. Large-scale cDNA transfection screening for genes related to cancer development and progression. *Proc Natl Acad Sci U S A* 2004;101:15724–9.
- Goldman P, Levy CC. The enzymatic hydrolysis of folate analogues. *Biochem Pharmacol* 1968;17:2265–70.
- Goldman P, Levy CC. Carboxypeptidase G: purification and properties. *Proc Natl Acad Sci U S A* 1967;58:1299–306.
- Ng IO, Lai EC, Fan ST, Ng MM, So MK. Prognostic significance of pathologic features of hepatocellular carcinoma. A multivariate analysis of 278 patients. *Cancer* 1995;76:2443–8.
- Kozak M. Adherence to the first-AUG rule when a second AUG codon follows closely upon the first. *Proc Natl Acad Sci U S A* 1995;92:2662–6.
- Breathnach R, Benoist C, O'Hare K, Gannon F, Chambon P. Ovalbumin gene: evidence for a leader sequence in mRNA and DNA sequences at the exon-intron boundaries. *Proc Natl Acad Sci U S A* 1978;75:4853–7.
- Mount SM. A catalogue of splice junction sequences. *Nucleic Acids Res* 1982;10:459–72.
- Barinka C, Mlcochova P, Sacha P, et al. Amino acids at the N- and C-termini of human glutamate carboxypeptidase II are required for enzymatic activity and proper folding. *Eur J Biochem* 2004;271:2782–90.
- Kogerman P, Sy MS, Culp LA. Overexpressed human *CD44s* promotes lung colonization during micrometastasis of murine fibrosarcoma cells: facilitated retention in the lung vasculature. *Proc Natl Acad Sci U S A* 1997;94:13233–8.
- Johnson LD, Hunt DM, Kim K, Nachtigal M. Amplification of stromelysin-3 transcripts from carcinomas of the colon. *Hum Pathol* 1996;27:964–8.
- Robledo MM, Bartolome RA, Longo N, et al. Expression of functional chemokine receptors *CXCR3* and *CXCR4* on human melanoma cells. *J Biol Chem* 2001;276:45098–105.
- Lindner HA, Lunin VV, Alary A, Hecker R, Cygler M, Menard R. Essential roles of zinc ligation and enzyme dimerization for catalysis in the aminocyclase-1/M20 family. *J Biol Chem* 2003;278:44496–504.
- Bonacchi A, Romagnani P, Romanelli RG, et al. Signal transduction by the chemokine receptor *CXCR3*: activation of Ras/ERK, Src, and phosphatidylinositol 3-kinase/Akt controls cell migration and proliferation in human vascular pericytes. *J Biol Chem* 2001;276:9945–54.
- Kawada K, Sonoshita M, Sakashita H, et al. Pivotal role of *CXCR3* in melanoma cell metastasis to lymph nodes. *Cancer Res* 2004;64:4010–7.
- Trentin L, Agostini C, Facco M, et al. The chemokine

- receptor CXCR3 is expressed on malignant B cells and mediates chemotaxis. *J Clin Invest* 1999;104:115–21.
17. Premack BA, Schall TJ. Chemokine receptors: gateways to inflammation and infection. *Nat Med* 1996;2:1174–8.
18. Rossi D, Zlotnik A. The biology of chemokines and their receptors. *Annu Rev Immunol* 2000;18:217–42.
19. Mellado M, Rodriguez-Frade JM, Manes S, Martinez AC. Chemokine signaling and functional responses: the role of receptor dimerization and TK pathway activation. *Annu Rev Immunol* 2001;19:397–421.
20. Boulay A, Masson R, Chenard MP, et al. High cancer cell death in syngeneic tumors developed in host mice deficient for the stromelysin-3 matrix metalloproteinase. *Cancer Res* 2001;61:2189–93.
21. Deng H, Guo RF, Li WM, Zhao M, Lu YY. Matrix metalloproteinase 11 depletion inhibits cell proliferation in gastric cancer cells. *Biochem Biophys Res Commun* 2005;326:274–81.
22. Naor D, Sionov RV, Ish-Shalom D. CD44: structure, function, and association with the malignant process. *Adv Cancer Res* 1997;71:241–319.
23. Miletti-Gonzalez KE, Chen S, Muthukumaran N, et al. The CD44 receptor interacts with P-glycoprotein to promote cell migration and invasion in cancer. *Cancer Res* 2005;65:6660–7.
24. Pereira PA, Rubenthiran U, Kaneko M, Jothy S, Smith AJ. CD44s expression mitigates the phenotype of human colorectal cancer hepatic metastases. *Anti-cancer Res* 2001;21:2713–7.
25. Yanagisawa N, Mikami T, Mitomi H, Saegusa M, Koike M, Okayasu I. CD44 variant overexpression in gallbladder carcinoma associated with tumor dedifferentiation. *Cancer* 2001;91:408–16.

Clinical Cancer Research

Identification of *Carboxypeptidase of Glutamate Like-B* as a Candidate Suppressor in Cell Growth and Metastasis in Human Hepatocellular Carcinoma

Pingping Zhang, David Wai Chan, YiYi Zhu, et al.

Clin Cancer Res 2006;12:6617-6625.

Updated version Access the most recent version of this article at:
<http://clincancerres.aacrjournals.org/content/12/22/6617>

Cited articles This article cites 25 articles, 12 of which you can access for free at:
<http://clincancerres.aacrjournals.org/content/12/22/6617.full#ref-list-1>

Citing articles This article has been cited by 3 HighWire-hosted articles. Access the articles at:
<http://clincancerres.aacrjournals.org/content/12/22/6617.full#related-urls>

E-mail alerts [Sign up to receive free email-alerts](#) related to this article or journal.

Reprints and Subscriptions To order reprints of this article or to subscribe to the journal, contact the AACR Publications Department at pubs@aacr.org.

Permissions To request permission to re-use all or part of this article, use this link
<http://clincancerres.aacrjournals.org/content/12/22/6617>.
Click on "Request Permissions" which will take you to the Copyright Clearance Center's (CCC) Rightslink site.